

Magnetotransport properties in the magnetic phase of $\text{BaFe}_{2-x}\text{T}_x\text{As}_2$ ($T = \text{Co, Ni}$): A magnetic excitations approach

J. P. Peña,¹ M. M. Piva,² P. F. S. Rosa,^{2,3} P. G. Pagliuso,² C. Adriano,² T. Grant,³ Z. Fisk,³ E. Baggio-Saitovitch,⁴ and P. Pureur¹

¹*Instituto de Física, Universidade Federal do Rio Grande do Sul, Avenida Bento Gonçalves 9500, 15051, 91501-970 Porto Alegre, Rio Grande do Sul, Brazil*

²*Instituto de Física Gleb Wataghin, Universidade Estadual de Campinas, Rua Sérgio Buarque de Holanda 777, 13083-970 Campinas, São Paulo, Brazil*

³*Department of Physics and Astronomy, School of Physical Sciences, University of California, 2186 Frederick Reines Hall, Irvine, California 92697-4574, USA*

⁴*Centro Brasileiro de Pesquisas Físicas, Rua Dr. Xavier Sigaud 150, 22290-180 Rio de Janeiro, Rio de Janeiro, Brazil*



(Received 31 October 2017; revised manuscript received 26 December 2017; published 5 March 2018)

Because of their complex Fermi surfaces, the identification of the physical phenomena contributing to electronic scattering in the Fe-based superconductors is a difficult task. Here, we report on the electrical resistivity, magnetoresistance, and Hall effect in two series of $\text{BaFe}_{2-x}\text{T}_x\text{As}_2$ ($T = \text{Co, Ni}$) crystals with different values of x . The T contents were chosen so that the majority of the investigated samples present an intermediate magnetically ordered state and a superconducting ground state. We interpret the obtained results in terms of scattering of charge carriers by magnetic excitations instead of describing them as resulting uniquely from effects related to multiple-band conduction. Our samples are single crystals from the structural point of view and their overall magnetotransport properties are dominated by a single magnetic state.

DOI: [10.1103/PhysRevB.97.104502](https://doi.org/10.1103/PhysRevB.97.104502)

I. INTRODUCTION

Electronic transport measurements are useful to survey the origin of electronic scattering and the excitation spectrum of a material's superficial and bulk states. However, in many cases several physical phenomena contribute to scattering events, so that the achievement of a correct and unique interpretation of the experimental results can become a major difficulty. The electrical magnetotransport properties of the Fe-based superconductors (FeSC) are representative of these complex cases. In most of these materials, the five different hole and electron bands forming the Fermi surface (FS) [1,2], and the exotic nematic/magnetic ordering established at the spin density wave (SDW) critical temperature, T_{SDW} , make it difficult to establish what are the main factors ruling the charge transport in these compounds.

In the parent compound of the 122 family, BaFe_2As_2 , both the transversal magnetoresistance (MR in the geometry $B \parallel c$ axis; $B \perp I$) and the Hall coefficient, R_H , exhibit unusual magnetic-field and temperature dependencies in the region $T < T_{\text{SDW}}$ [3–7]. In particular, the absolute values of the MR and R_H sharply increase when the temperature decreases below T_{SDW} . These effects are commonly explained in the context of multiple-band conduction models [5,6,8]. Such models require variations in the number and mobility of the charge carriers all along the SDW phase. Those variations are partially justified by the expected opening of a SDW-type gap. In fact, infrared and optical spectroscopy measurements show that a spectral weight loss appears in the low-energy spectrum of BaFe_2As_2 below $T = T_{\text{SDW}}$ [9,10]. Nonetheless, angle resolved photoemission spectroscopy (ARPES) results do not support the opening of an actual gap in the Fermi surface

[11]. Instead, a severe reorganization of the bands and the emergence of singular strong Fermi spots are observed [11]. This reorganization of the bands provides additional channels for interband transitions which could offer an interpretation of the optical results different than that based on the opening of a SDW gap [11]. Additional ARPES results in Ref. [12] show that the electronic reconstruction below T_{SDW} is highly orbital dependent. That characteristic makes the $\text{Fe-}3d_{xz}$ band dominant over the other iron bands in the magnetic phase [12], contrasting with the more multiorbital character of the paramagnetic (PM) phase. In conclusion, ARPES results seem to remove some of the importance given to the gap opening and multiple band character to explain the transport phenomena in the SDW phase of the FeSC.

Concerning the magnetic ordering, the multiple-band models consider that the Fe-based pnictides are well described by a fully itinerant picture where the opening of a normal SDW gap plays the major role. However, many works point out that both itinerant and localized nature of the magnetic moments have to be taken into account to properly describe the magnetic, transport, and spectroscopic properties of these compounds [10,11,13–15]. In fact, by analyzing ARPES results, authors in Ref. [16] affirm that one could visualize the magnetic phase in BaFe_2As_2 within the perspective of effective local moments, so that the collinear SDW order is caused by the exchange interactions between the nearest neighbors and the next-nearest neighbors. Within this scenario, the SDW naturally becomes commensurate in the parent compound without requiring the opening of a large gap on the Fermi surface or nesting of the hole and electron bands [16]. In consequence, evoking the partially local character of magnetic moments and the fact that magnetic excitations can strongly modify a material's

TABLE I. Characterization parameters of the main electronic phase of the samples studied here. NM denotes “Not measured.”

Sample	$T = \text{Co}$			Sample	$T = \text{Ni}$		
	c (Å)	x	T_{SDW} (K)		c (Å)	x	T_{SDW} (K)
Co-A	13.028(2)	0.023(2)	119(1)	Ni-A	13.058(2)	0.015(2)	121(1)
Co-B	13.003(2)	0.032(3)	115(2)	Ni-B	13.018(2)	0.030(2)	105(2)
Co-C	13.013(2)	0.037(4)	113(4)	Ni-C	13.038(2)	0.033(2)	101(3)
Co-D	13.034(2)	0.043(4)	108(2)	Ni-D	13.011(2)	0.035(2)	98(3)
Co-E	12.979(2)	0.118(2)	70(2)	Ni-E	NM	0.051(4)	67(3)

quasiparticle scattering spectrum, some authors proposed that carrier scattering by magnetic excitations plays an additional, relevant mechanism for completely describing the magneto-transport properties of the Fe-based pnictides, including the T -substituted systems [7,17].

Here we analyze the magnetotransport properties of two series of $\text{BaFe}_{2-x}\text{T}_x\text{As}_2$ samples, with $T = \text{Co}$ and Ni. The T content was varied within a range where the SDW ordering is preserved in all studied crystals. Most of these samples have a superconducting ground state, which is not necessarily associated with the same phase provoking the magnetically ordered phase. We show that the exotic behavior of the magnetotransport properties exhibited by the BaFe_2As_2 is displaced to lower temperatures in the T -substituted samples. Even so, the striking differences between these properties in the PM and SDW phases remain while a magnetically ordered phase is manifested. We argue that the description of the essential changes observed in the magnetotransport properties of the studied samples in the magnetically ordered state is mostly due to carrier scattering by magnetic excitations, although the effects from the multiple-band character of the charge carriers and the Fermi-surface reconstruction phenomenon cannot be ignored.

II. EXPERIMENTAL DETAILS

Crystals of $\text{BaFe}_{2-x}\text{T}_x\text{As}_2$ ($T = \text{Co}, \text{Ni}$) were synthesized by the autoflux or by the In-flux methods. The complete synthesis processes are reported in Refs. [18,19]. Energy dispersive spectroscopy (EDS), x-ray diffraction (XRD), and resistivity versus temperature (four-probe method) measurements were performed in all samples for characterization. We were not able to calculate the x value from the EDS results in all cases. Then, the content of Co or Ni atoms was estimated by a comparison of the transition temperatures (magnetic and superconducting) identified in the electrical resistivity curves with phase diagrams in literature [19–21]. From XRD patterns we could identify only one crystalline phase from the recorded $(00l)$ peaks of the $\text{Cu}k_{\alpha 1}$ and $\text{Cu}k_{\alpha 2}$ diffractions. Despite the single-crystal character of the samples, the zero-field electrical resistivity curves revealed in some cases more than one magnetic or superconducting critical temperature. We attribute these features to the presence of minority phases with different contents of the T atoms or partial superficial oxidation. This effect is probably present, but went unnoticed, in several samples of the 122 family of the Fe-based superconductors presenting simultaneously magnetic and superconducting states. Nevertheless, the highest magnetic transition temperature,

labeled as T_{SDW} and associated with a remarkable resistivity anomaly, characterizes the largely dominant electronic phase in all cases. Table I summarizes the parameters characterizing the main phase of the ten studied samples (in five of these samples $T = \text{Co}$, and in the other five $T = \text{Ni}$). These parameters are the c -axis lattice length, the T content of the dominant electronic phase, and the respective ordering temperature T_{SDW} .

The electrical transport measurements were carried out with the four-probe method in a low-frequency ac bridge of a commercial Quantum Design physical property measurement system platform. Two contacts pads for current were attached with silver epoxy to the extremities of samples having the approximate form of parallelepipeds. Two contact leads were attached to the same (opposite) edge of the sample for measuring the longitudinal (transversal) voltage. Magnetic fields with magnitude in the range $B = 0$ and ± 9 T were applied parallel to the c axis and perpendicularly to the current. The planar component of the magnetoresistance and the Hall resistivity were determined from the averages $\rho_{\text{even}} = \frac{\rho_{++} + \rho_{--}}{2}$ and $\rho_{\text{odd}} = \frac{\rho_{+-} - \rho_{-+}}{2}$ of the longitudinal and transversal measurements, respectively. The term $\rho_{+/-}$ refers to the resistivity measured when the direction of the magnetic field was positive/negative with respect to the vertical axis.

III. RESULTS AND DISCUSSION

A. Resistivity

Panels (a) and (b) of Fig. 1 show the electrical resistivity as a function of the temperature for the series of samples with $T = \text{Co}$ and Ni, respectively. A prominent feature in these results is the marked increase of the resistivity below the characteristic temperature denoted as T_{SDW} . The observed hump recalls the superzone effect related to the opening of a gap in the conduction band due to the antiferromagnetic ordering [22–24]. The gap and the associated Fermi-surface

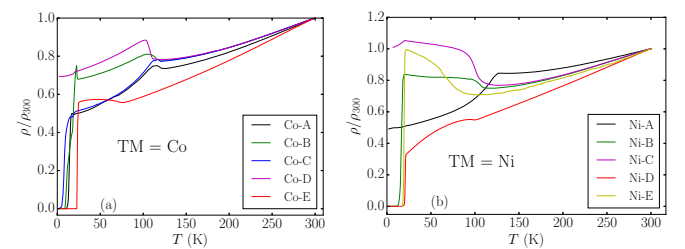


FIG. 1. Resistivity as a function of the temperature for the series of samples partially substituted with (a) $T = \text{Co}$ and (b) $T = \text{Ni}$. In both cases the resistivity is normalized by its value in $T = 300$ K.

distortion are expected to occur when the periodicity of the magnetic lattice does not coincide with that of the atomic lattice. This effect is commonly observed closely below the Néel temperature of antiferromagnetic metals, as Cr [25], Mn [26], and some of the heavy rare earths [27]. In the FeSC, that incommensurability probably occurs because of the nematicity observed together with the SDW ordering [1]. At this point it is worth noting that the superzone effect is not so evident in the BaFe_2As_2 parent compound. In the BaFe_2As_2 the opening of a gap driving an effective reduction of the electronic density in the ordered phase tends to be compensated by a higher mobility due to coherent scattering; thus, a nonmetal behavior of the ρ versus T curve is observed in a very small region. In the substituted specimens, where the structural transition occurs at $T = T_S$ such that $T_S > T_{SDW}$ [28], an increasing resistivity is already observed below T_S , and it continues to grow below T_{SDW} until $T = T_c$. This implies that the T substitution disrupts the commensurability of the SDW ordering leading to an enhanced region where the superzone effect is observed in the substituted samples with respect to that of the pure compound. In this scenario, the main role of the structural transition is to remove the commensurability of the magnetic and structural lattices and this, together with the scattering by magnetic excitations, gives origin to the hump in the resistivity.

In the results of Fig. 1, one observes that the Ni atoms depress T_{SDW} more efficiently than Co in similar quantities. The qualitative comparison between results in Figs. 1(a) and 1(b) also suggests that Ni disturbs the coherent carrier scattering by magnetic excitations more than Co. Indeed, the resistivity in the $\text{BaFe}_{2-x}\text{Ni}_x\text{As}_2$ compounds shows a marked tendency to stay constant below T_{SDW} , whereas in the systems with $T = \text{Co}$ ρ decreases neatly below the magnetic ordering temperature because of the continuous reduction of thermal induced spin disorder. It should be noted, however, that neither Co nor Ni introduces localized magnetic moments in $\text{BaFe}_{2-x}\text{TxAs}_2$ [29,30]. Then, the main role of both scatterers seems to disrupt the SDW ordered state characteristic of the parent compound.

B. Magnetoresistance

The MR is given as the quotient $\frac{\Delta\rho}{\rho(0)} = \frac{\rho(B) - \rho(0)}{\rho(0)}$. In Figs. 2(a) and 2(b), measurements of the MR as a function of the magnetic field in several fixed temperatures are shown for representative samples of the Co and Ni substituted series, respectively. The MR behaves as a power law of the applied field, $\Delta\rho = aB^b$, with $b \simeq 3/2$, much like previously observed in slightly substituted samples [7].

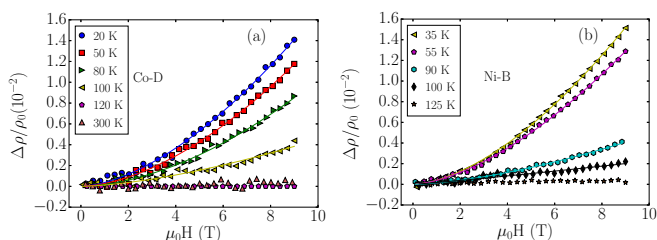


FIG. 2. Magnetoresistance as a function of the magnetic field in several fixed temperatures for samples Co-D ($x = 0.043$) and Ni-B ($x = 0.030$). Solid lines are fits to equation $\Delta\rho = aB^b$, with $b \simeq 3/2$.

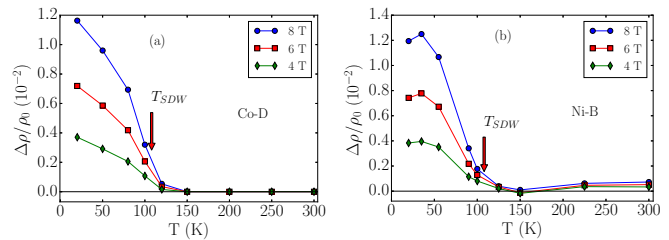


FIG. 3. MR amplitudes in several fixed fields plotted as a function of the temperature for samples (a) Co-D ($x = 0.043$) and (b) Ni-B ($x = 0.030$) in panel (b).

In Figs. 3(a) and 3(b) the MR amplitude in three fixed fields is shown as a function of the temperature for the same samples of Fig. 2. In both cases, one observes the striking resemblance of the MR amplitude with an order parameter which becomes measurable only below the transition temperature T_{SDW} .

In the two-band model the MR is given by [31]

$$\Delta\rho \approx \frac{\sigma_h\sigma_e(\mu_h - \mu_e)^2}{(\sigma_h + \sigma_e)^2} H^2, \quad (1)$$

where $\sigma_{h(e)}$ is the conductivity of the hole (electron) band and $\mu_{h(e)}$ is the respective mobility. The small MR observed above T_{SDW} in both panels of Fig. 3 can be explained within this model assuming the presence of two types of carriers with similar mobilities. This is a reasonable assumption taking into account experimental results showing that both electron and hole bands contribute equally to the charge transport in most of the phase diagram of the FeSC of the 122 family [6,32].

On the other hand, the validity of Eq. (1) in the magnetically ordered state would require a MR quadratically dependent on the field and a large difference between the mobilities of the hole and electron bands. The first requirement is not fulfilled by the experimental data. The second would imply that abrupt and drastic changes have to occur in the Fermi surface of electron doped FeSC, with suppression of the hole pocket, because of the magnetic ordering. Indeed, a reconstruction of the FS occurs at $T = T_{SDW}$ because of the SDW gap opening. However, this effect is not expected to produce strong changes in the hole and electron mobilities [12]. On the other hand, it has been argued that a significant modification of the Fermi surface in electron doped FeSC with suppression of the hole pocket may occur because of a Lifshitz transition accompanying the magnetic ordering at T_{SDW} . Again, this argument must be confronted with the fact that optical spectroscopy and ARPES measurements suggest that the proposed Lifshitz transition occurs only in pure and heavily underdoped samples of the 122 Fe-pnictides system [9,33,34]. Thus, assuming that holes are removed because of a Lifshitz transition and MR is enhanced according to Eq. (1) would leave the behavior of the magnetoresistance unexplained in most of our samples, which are not in the T concentration limit where the topological effect has been proposed to set in (this is true independently of T being Co or Ni). Moreover, since there is no order parameter associated with a topological Lifshitz transition, to explain the temperature dependence of the MR as shown in Fig. 3 solely based on this concept does not follow straightforwardly. Finally, even considering that the main changes in the electronic structure observed in spectroscopic measurements can be taken

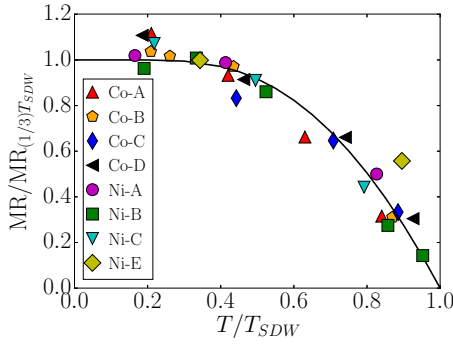


FIG. 4. MR amplitude normalized to its value at $T = (1/3)T_{SDW}$ as a function of the normalized temperature T/T_{SDW} for the Co- and Ni-substituted series of samples. The solid line represents the square of the Brillouin function for $J = 1/2$ (see text).

as originated by interband phenomena developing near the Γ pocket, one cannot exclude the possibility that the charge carriers are strongly interacting with magnetic, orbital, or nematic fluctuations [9]. These facts suggest that an additional and quantitatively more relevant mechanism, other than the multiple-band conduction, must be taken into consideration to fully explain the magnetotransport properties of the 122 Fe pnictides. We then propose that electron scattering by magnetic excitations has an important role to explain the MR in the magnetically ordered region of our samples.

In order to seek experimental evidences supporting our assumption, in Fig. 4 we plot the MR amplitude at $B = 8$ T, normalized to its value at $T = \frac{1}{3}T_{SDW}$, as a function of the reduced temperature T/T_{SDW} for both series of samples studied here. The black continuous line represents the square of the normalized staggered magnetization as a function of the temperature, as described by the Brillouin function for $J = 1/2$. This value for J coincides with the value calculated for the effective local spin, S_{eff} , in the spin-state crossover model in Ref. [35]. That effective spin arises from the dynamical mixing of the quasidegenerate spin states of Fe^{2+} ions by intersite electron hoppings [35]. The collapse of the data for both families of samples over the line predicted by the mean field theory is remarkable, and suggests that this theory is roughly valid and the magnetoresistance is proportional to the square of the staggered magnetization. Moreover, this clearly indicates a universal scaling between the MR value with T_{SDW} in the FeSC of the 122 family. There are, however, two exceptions to this universal scaling: these are the samples Co-E and Ni-D. We argue this can indicate that the effects of the magnetic ordering in the resistivity and MR are quite weak for these two specimens.

C. Hall effect

In Fig. 5 we show representative transversal resistivity curves (ρ_{xy} versus H) for two of the studied samples of $BaFe_{2-x}T_xAs_2$. Namely, results for samples Co-C ($x = 0.037$) and Ni-C ($x = 0.033$) are shown in panels (a) and (b), respectively. The same linear behavior of ρ_{xy} as a function of the field was observed for all samples in the complete temperature interval investigated (except for measurements performed very close to the superconducting critical temperature). Thus, in all

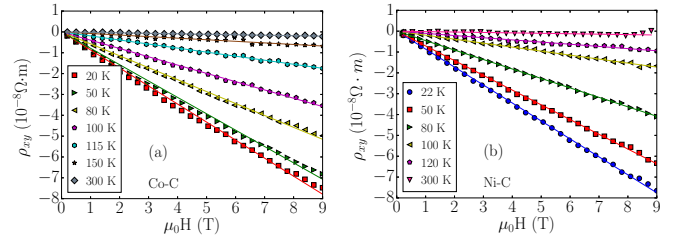


FIG. 5. Hall resistivity as a function of the applied field for the samples (a) Co-C ($x = 0.037$) and (b) Ni-C ($x = 0.033$). The experimental data are fitted to straight lines.

cases the Hall coefficient R_H was calculated as the slope of those straight lines.

The Hall coefficient R_H is presented as a function of the temperature in Fig. 6 for the series of samples where $T = Co$ in panel (a) and $T = Ni$ in panel (b). The most conspicuous characteristic of curves in Fig. 6 is the strong change in the magnitude and temperature dependence of R_H at $T = T_{SDW}$. Above T_{SDW} the Hall coefficient is small and weakly temperature dependent. Below T_{SDW} , the magnitude of R_H increases sharply. As for the MR, the small value of R_H in the PM regime can be explained by a simple two-band model with two almost compensated bands of similar mobilities, as expressed by the equation [31]

$$R_H \approx \frac{\sigma_h \mu_h - \sigma_e \mu_e}{(\sigma_h + \sigma_e)^2}. \quad (2)$$

Once again, assuming the hypothesis that the two-band model is enough to explain the strongly different magnitude and temperature dependence of R_H in the magnetically ordered region demands a drastic reduction in the hole-type carrier density, as assumed in Ref. [5], or significant and opposite changes in the mobilities of electrons and holes, as supposed in Refs. [6,32]. Indeed, it might be tempting to consider that a severe Fermi-surface reconstruction (Lifshitz transition) occurring at $T = T_{SDW}$ triggers a large and continuous change in the magnitude of the carrier density in the magnetically ordered phase of the Fe pnictides when compared to that of the PM state. For example, ARPES measurements and theoretical calculations in Ref. [36] support the existence of an unexpected temperature dependence of the Fermi-surface geometry in $BaFe_{2-x}Co_xAs_2$ samples. However, the study in Ref. [36] is focused on samples corresponding to the overdoped side of the dome. These samples do not present a magnetically ordered phase.

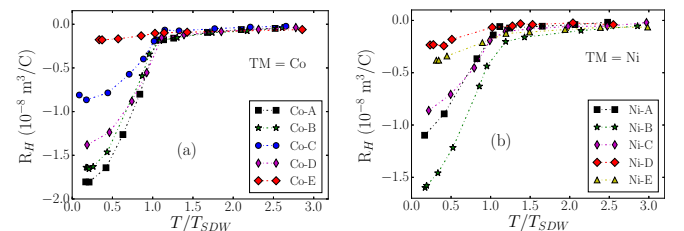


FIG. 6. Hall coefficient as a function of the temperature for samples with (a) $T = Co$ and (b) $T = Ni$. The values for R_H were extracted from the slope of linear fittings of plots as those shown in Fig. 5.

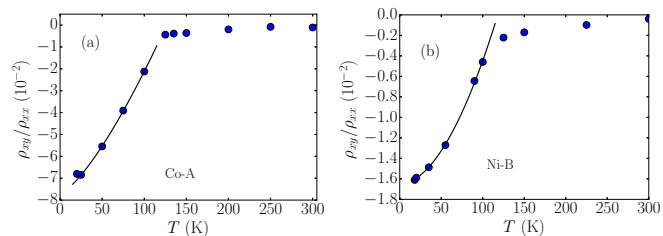


FIG. 7. Tangent of the Hall angle for the samples (a) Co-A ($x = 0.023$) and (b) Ni-B ($x = 0.030$). Both data sets are for a fixed magnetic field of magnitude 4 T.

Moreover, results reported by these authors for the undoped compound do not hint at evidences for a severe loss of carriers at $T = T_{\text{SDW}}$. Conversely, the numbers of carriers obtained by them at $T \sim 0$ and $T = 200$ K are almost the same [36].

Other experimental studies, which analyze samples covering a larger region of the phase diagram and focus on the differences among the properties of the PM and SDW phases, conclude that a Lifshitz transition occurs in specimens where the T content is about or below that characterizing the emergence of the superconducting dome [34,37]. However, our results and other Hall effect results [5,6,32] show that the qualitative behavior of the R_H versus T curves is preserved whenever a magnetically ordered phase is observed, independently of the T content. Therefore, the hypothesis evoking the loss of carriers due to the occurrence of a Lifshitz transition at $T = T_{\text{SDW}}$ may not apply to explain the sharp increase in the R_H magnitude observed below this point in samples spanning a large part of the phase diagram. As for the MR, the above considerations lead us to propose that the interaction of the charge carriers with magnetic excitations should also be considered to fully describe the Hall effect behavior in the FeSC where an intermediate magnetic phase is present. In other terms, the Hall coefficient should have its temperature dependence attributed to an anomalous term of magnetic origin that comes into play in temperatures below T_{SDW} .

As a final insight, in panels (a) and (b) of Fig. 7 we plot the tangent of the Hall angle, $\tan \Theta_H = \rho_{xy}/\rho_{xx}$, as a function of the temperature for representative Co-substituted and Ni-substituted samples, respectively. Fittings of the Hall angle to a function of the form

$$\tan \Theta_H = \alpha + \beta T^n \quad (3)$$

are presented as solid black lines and the fitting coefficients and exponents are listed for all samples in Table II. Results in Fig. 7 may be compared to those published in Ref. [7].

One then observes that $\tan \Theta_H(T)$ evolves from a linear function of the temperature in the slightly substituted, and non-superconducting, samples [7] to an approximately quadratic temperature behavior in samples with higher T content, for which a superconducting ground state is stabilized. It is also shown in the results of Fig. 7 that $\tan \Theta_H$ tends to zero as the superconducting transition is approached from above.

From data in Table II one observes that (i) when $T \rightarrow 0$ there is a nonzero contribution to the Hall tangent represented by the parameter α ; (ii) the parameter α is, in general, higher in samples with lower T content; and (iii) the absolute values for α are higher for the Co-substituted samples than for the Ni-substituted ones. In Table II it is also possible to see that the parameter β almost vanishes in samples with the weakest magnetic order in both series of samples. The first point strongly suggests that a noncollinear spin structure or some quenched magnetic disorder is present in the investigated samples. This contribution is normally associated with spin chirality [38,39]. The second and third points suggest that the chiral mechanism, present in samples with the most robust magnetic ordering, is diminished when that ordering is disturbed via the augmentation of the T content. The temperature-dependent term in Eq. (3) is rather related to skew scattering produced by individual spins [38,39]. This term also shows a tendency to vanish when x is increased, thus revealing the gradual weakening of the intermediate magnetic order as the T content increases. We thus propose that the temperature and x dependence of $\tan \Theta_H$ in the $\text{BaFe}_{2-x}\text{T}_x\text{As}_2$ compounds are related to anomalous contribution to the Hall effect that has its origin in noncollinear and localized magnetic moments that coexist with the itinerant ones [13,14,40] responsible for the SDW arrangement.

IV. FINAL COMMENTS AND CONCLUSIONS

The importance of the scattering by magnetic fluctuations to the transport properties of Fe-based 122 pnictides, superconducting or not, has been pointed out in previous works [7,41,42]. For example, the anisotropic resistance in the nematic phase has been described with an Ising-nematic model where the anisotropy is the product of the interference between scattering by impurities and by critical spin fluctuations [41]. Such a model emerges from the combination of magnetic fluctuations and frustration [41]. On the other hand, multiple-band conduction models reproduce experimental resistance curves of FeSC in the absence of an external magnetic field [17,43]. Nevertheless these models are not able to adequately describe the magnetotransport properties in the

TABLE II. Parameters obtained from fittings of $\tan \Theta_H$ to Eq. (3) in the region $T < T_{\text{SDW}}$ for both series of studied samples.

$T = \text{Co}$				$T = \text{Ni}$			
x	$\alpha \times 10^{-3}$	$\beta \times 10^{-5}$	n	x	$\alpha \times 10^{-3}$	$\beta \times 10^{-5}$	n
0.023	-77 ± 1	10.00 ± 2.0	1.36 ± 0.04	0.015	-31 ± 1	13.0 ± 1.00	1.13 ± 0.01
0.032	-40 ± 1	0.90 ± 0.4	1.80 ± 0.10	0.030	-16 ± 1	0.12 ± 0.09	1.90 ± 0.10
0.037	-78 ± 2	4.00 ± 2.0	1.60 ± 0.10	0.033	-11 ± 1	0.08 ± 0.01	1.95 ± 0.01
0.043	-53 ± 1	0.80 ± 0.5	1.80 ± 0.10	0.035	-15 ± 1	0.27 ± 0.04	2.00 ± 0.10
0.118	-6 ± 1	0.03 ± 0.0	2.10 ± 0.01	0.051	-5 ± 1	0.05 ± 0.01	2.00 ± 0.10

SDW phase of those compounds without assuming a restrictive hypothesis on the mobility and/or number of the charge carriers. Thus, it seems that considering that the multiple-band models are able to fully describe the magnetotransport properties of the FeSC is not entirely justified on experimental grounds. Lifshitz transitions and exotic temperature-dependent Fermi surfaces explain only partially the behavior of the MR and Hall coefficient. Our previous results in slightly doped and nonsuperconducting samples [7] as well as the results of this paper in samples having a superconducting ground state while preserving an intermediate magnetic phase reveal that, once a magnetic transition occurs, large changes in the absolute values and temperature dependence of MR and the Hall coefficient are observed in the region $T \leq T_{\text{SDW}}$, independently of the T substitution or of how low T_{SDW} is.

Accumulative experimental evidences show that Fermi-surface reconstructions are only observed in the pure and slightly substituted samples ($\sim 20\%$) [33,44]. On the other hand, although temperature-dependent energy bands have been considered as an intrinsic characteristic of the 122 system, this peculiarity was not related with the existence of a magnetically ordered phase [44]. Then, this effect may not be considered as the unique mechanism to explain the striking differences of the magnetotransport properties of underdoped samples above and below T_{SDW} . Taking into account that the iron-pnictogen distance controls the overlap between iron and pnictogen orbitals, enforcing iron electrons to become more localized with increasing distance [15], the fact that the c -axis lattice parameter decreases with addition of T atoms in the doped compounds implies that itinerancy increases with doping. In the context of scattering by magnetic fluctuations, this scenario agrees with the fact that in pure and slightly doped samples a much stronger variation of MR and R_H is observed below T_{SDW} than in optimally doped and overdoped samples. This happens because of the more localized character of magnetic moments in the small x limit. We can then speculate that the

itinerant electrons are rather responsible for the multiple-band effects in the electron transport properties of the 122-FeSC compounds while more localized electrons are responsible for the anomalous MR and Hall effect components.

In summary, we have studied two series of $\text{BaFe}_{2-x}\text{T}_x\text{As}_2$ crystals, where $T = \text{Co}$ and Ni . While presenting an intermediate magnetic state, most of our samples have a superconducting ground state. The superconducting transition temperatures do not always match with the magnetic ordering temperature T_{SDW} for the dominant phase, indicating that some phase separation occurs in the studied samples.

We interpret the characteristic hump of the resistivity occurring at T_{SDW} as a superzone effect, which means that not only does some reconstruction of the Fermi surface occur at this temperature due to the stabilization of an anti-ferromagnetic-like state but intense scattering by magnetic excitations plays a major role. We also proposed that the sharp increase of the MR amplitude observed in the magnetically ordered phase, and its universal scaling with the reduced temperature T/T_{SDW} , indicate that this magnetotransport property is rather related with scattering of carriers by magnetic excitations than with drastic changes in the mobility or density of the charge carriers. Finally, our Hall effect results suggest that anomalous terms related to magnetic excitations contribute to the Hall resistivity of all the studied samples in the magnetically ordered phase. This contribution is progressively weakened upon increasing the Co or Ni concentration.

ACKNOWLEDGMENTS

This work was partially financed by the Brazilian agencies FAPERGS (PRONEX Grant No. 12/2014), FAPESP (Grants No. 2012/05903-6, No. 2012/04870-7, and No. 2011/01564-0), and CNPq (PRONEX Grants No. 12/2014, No. 304649/2013-9, and No. 442230/2014-1). J.P.P. benefits from a PNPd/CAPES fellowship.

-
- [1] J. Paglione and R. Greene, *Nat. Phys.* **6**, 645 (2010).
 [2] K. Ishida, Y. Nakai, and H. Hosono, *JPSJ* **78**, 062001 (2009).
 [3] H.-H. Kuo, J.-H. Chu, S. C. Riggs, Leo Yu, P. L. McMahon, K. De Greve, Y. Yamamoto, J. G. Analytis, and I. R. Fisher, *Phys. Rev. B* **84**, 054540 (2011).
 [4] K. K. Huynh, Y. Tanabe, and K. Tanigaki, *Phys. Rev. Lett.* **106**, 217004 (2011).
 [5] F. Rullier-Albenque, D. Colson, A. Forget, and H. Alloul, *Phys. Rev. Lett.* **103**, 057001 (2009).
 [6] L. Fang, H. Luo, P. Cheng, Z. Wang, Y. Jia, G. Mu, B. Shen, I. I. Mazin, L. Shan, C. Ren, and H.-H. Wen, *Phys. Rev. B* **80**, 140508(R) (2009).
 [7] J. P. Peña, M. M. Piva, C. B. R. Jesus, G. G. Lesseux, T. M. Garitezi, D. Tobia, P. F. S. Rosa, T. Grant, Z. Fisk, C. Adriano, R. R. Urbano, P. G. Pagliuso, and P. Pureur, *Physica C* **531**, 30 (2016).
 [8] M. Yi, D. H. Lu, J. G. Analytis, J.-H. Chu, S.-K. Mo, R.-H. He, M. Hashimoto, R. G. Moore, I. I. Mazin, D. J. Singh, Z. Hussain, I. R. Fisher, and Z.-X. Shen, *Phys. Rev. B* **80**, 174510 (2009).
 [9] P. Marsik, C. N. Wang, M. Rössle, M. Yazdi-Rizi, R. Schuster, K. W. Kim, A. Dubroka, D. Munzar, T. Wolf, X. H. Chen, and C. Bernhard, *Phys. Rev. B* **88**, 180508(R) (2013).
 [10] Z. P. Yin, K. Haule, and G. Kotliar, *Nat. Phys.* **7**, 294 (2011).
 [11] G. Liu, H. Liu, L. Zhao, W. Zhang, X. Jia, J. Meng, X. Dong, J. Zhang, G. F. Chen, G. Wang, Y. Zhou, Y. Zhu, X. Wang, Z. Xu, C. Chen, and X. J. Zhou, *Phys. Rev. B* **80**, 134519 (2009).
 [12] T. Shimojima, K. Ishizaka, Y. Ishida, N. Katayama, K. Ohgushi, T. Kiss, M. Okawa, T. Togashi, X.-Y. Wang, C.-T. Chen, S. Watanabe, R. Kadota, T. Oguchi, A. Chainani, and S. Shin, *Phys. Rev. Lett.* **104**, 057002 (2010).
 [13] J. Zhao, D. T. Adroja, D.-X. Yao, R. Bewley, Shiliang Li, X. F. Wang, G. Wu, X. H. Chen, J. Hu, and P. Dai, *Nat. Phys.* **5**, 555 (2009).
 [14] M. Liu, L. W. Harriger, H. Luo, M. Wang, R. A. Ewings, T. Guidi, H. Park, K. Haule, G. Kotliar, S. M. Hayden, and P. C. Dai, *Nat. Phys.* **8**, 376 (2012).
 [15] Z. P. Yin, K. Haule, and G. Kotliar, *Nat. Mater.* **10**, 932 (2011).
 [16] L. X. Yang, Y. Zhang, H. W. Ou, J. F. Zhao, D. W. Shen, B. Zhou, J. Wei, F. Chen, M. Xu, C. He, Y. Chen, Z. D. Wang,

- X. F. Wang, T. Wu, G. Wu, X. H. Chen, M. Arita, K. Shimada, M. Taniguchi, Z. Y. Lu, T. Xiang, and D. L. Feng, *Phys. Rev. Lett.* **102**, 107002 (2009).
- [17] M. J. Eom, S. W. Na, C. Hoch, R. K. Kremer, and J. S. Kim, *Phys. Rev. B* **85**, 024536 (2012).
- [18] T. M. Garitezi, C. Adriano, P. F. S. Rosa, E. M. Bittar, L. Bufaical, R. L. de Almeida, E. Granado, T. Grant, Z. Fisk, M. A. Avila, R. A. Ribeiro, P. L. Kuhns, A. P. Reyes, R. R. Urbano, and P. G. Pagliuso, *Braz. J. Phys.* **43**, 223 (2013).
- [19] Y. Chen, X. Lu, M. Wang, H. Luo, and S. Li, *Supercond. Sci. Technol.* **24**, 065004 (2011).
- [20] P. C. Canfield, S. L. Bud'ko, Ni Ni, J. Q. Yan, and A. Kracher, *Phys. Rev. B* **80**, 060501(R) (2009).
- [21] C. Canfield and S. L. Bud'ko, *Annu. Rev. Condens. Matter Phys.* **1**, 27 (2010).
- [22] A. R. Mackintosh, *Phys. Rev. Lett.* **9**, 90 (1962).
- [23] R. J. Elliott and F. A. Wedgwood, *Proc. Phys. Soc. London* **81**, 846 (1963).
- [24] H. Miwa, *Progr. Theoret. Phys. (Kyoto)* **29**, 477 (1963).
- [25] S. Araj, R. V. Colvin, and M. J. Marcinkowski, *J. Less Common Metals* **4**, 46 (1962).
- [26] G. T. Meaden and P. Pelloux-Gervais, *Cryogenics* **5**, 227 (1966).
- [27] S. Legvold, in *Magnetic Properties of Rare Earth Metals*, edited by R. J. Elliott (Plenum, London, 1972), p. 335.
- [28] J.-H. Chu, J. G. Analytis, C. Kucharczyk, and I. R. Fisher, *Phys. Rev. B* **79**, 014506 (2009).
- [29] F. S. Rosa, C. Adriano, T. M. Garitezi, M. M. Piva, K. Mydeen, T. Grant, Z. Fisk, M. Nicklas, R. R. Urbano, R. M. Fernandes, and P. G. Pagliuso, *Scientific Reports* **4**, 6252 (2014).
- [30] T. M. Garitezi, G. G. Lesseux, P. F. S. Rosa, C. Adriano, A. P. Reyes, P. L. Kuhns, P. G. Pagliuso, and R. R. Urbano, *J. Appl. Phys.* **115**, 17D711 (2014).
- [31] J. M. Ziman, *Principles of the Theory of Solids*, 2nd ed. (Cambridge University, Cambridge, England, 1972).
- [32] A. Olariu, F. Rullier-Albenque, D. Colson, and A. Forget, *Phys. Rev. B* **83**, 054518 (2011).
- [33] R. S. Dhaka, Chang Liu, R. M. Fernandes, Rui Jiang, C. P. Strehlow, Takeshi Kondo, A. Thaler, J. Schmalian, S. L. Budko, P. C. Canfield, and A. Kaminski, *Phys. Rev. Lett.* **107**, 267002 (2011).
- [34] C. Liu, T. Kondo, R. M. Fernandes, A. D. Palczewski, E. D. Mun, Ni Ni, A. N. Thaler, A. Bostwick, E. Rotenberg, J. Schmalian, S. L. Bud'ko, P. C. Canfield, and A. Kaminski, *Nat. Phys.* **6**, 419 (2010).
- [35] J. Chaloupka and G. Khaliullin, *Phys. Rev. Lett.* **110**, 207205 (2013).
- [36] V. Brouet, P.-H. Lin, Y. Texier, J. Bobroff, A. Taleb-Ibrahimi, P. Le Fèvre, F. Bertran, M. Casula, P. Werner, S. Biermann, F. Rullier-Albenque, A. Forget, and D. Colson, *Phys. Rev. Lett.* **110**, 167002 (2013).
- [37] E. D. Mun, S. L. Bud'ko, N. Ni, A. N. Thaler, and P. C. Canfield, *Phys. Rev. B* **80**, 054517 (2009).
- [38] N. Nagaosa, J. Sinova, S. Onoda, A. H. MacDonald, and N. P. Ong, *Rev. Mod. Phys.* **82**, 1539 (2010).
- [39] N. A. Sinitsyn, *J. Phys. Condens. Matter* **20**, 023201 (2008).
- [40] H. Gretarsson, A. Lupascu, J. Kim, D. Casa, T. Gog, W. Wu, S. R. Julian, Z. J. Xu, J. S. Wen, G. D. Gu, R. H. Yuan, Z. G. Chen, N.-L. Wang, S. Khim, K. H. Kim, M. Ishikado, I. Jarrige, S. Shamoto, J.-H. Chu, I. R. Fisher, and Y.-J. Kim, *Phys. Rev. B* **84**, 100509 (2011).
- [41] R. M. Fernandes, E. Abrahams, and J. Schmalian, *Phys. Rev. Lett.* **107**, 217002 (2011).
- [42] Y. Wang, M. N. Gastiasoro, B. M. Andersen, M. Tomić, H. O. Jeschke, R. Valentí, I. Paul, and P. J. Hirschfeld, *Phys. Rev. Lett.* **114**, 097003 (2015).
- [43] S. Ishida, T. Liang, M. Nakajima, K. Kihou, C. H. Lee, A. Iyo, H. Eisaki, T. Kakeshita, T. Kida, M. Hagiwara, Y. Tomioka, T. Ito, and S. Uchida, *Phys. Rev. B* **84**, 184514 (2011).
- [44] R. S. Dhaka, S. E. Hahn, E. Razzoli, Rui Jiang, M. Shi, B. N. Harmon, A. Thaler, S. L. Budko, P. C. Canfield, and A. Kaminski, *Phys. Rev. Lett.* **110**, 067002 (2013).